

4
15000
APR 1953
AUSTIN
WASH

MEASUREMENT OF BOUNDARY-LAYER TRANSITION ON A
STANDARD MODEL TO DETERMINE THE RELATIVE DISTURBANCE
LEVEL IN TWO SUPERSONIC WIND TUNNELS

19 FEBRUARY 1953



**U. S. NAVAL ORDNANCE LABORATORY
WHITE OAK, MARYLAND**

UNCLASSIFIED
NAVORD Report 2752

Aeroballistic Research Report 170

MEASUREMENT OF BOUNDARY-LAYER TRANSITION ON A
STANDARD MODEL TO DETERMINE THE RELATIVE DISTURBANCE
LEVEL IN TWO SUPERSONIC WIND TUNNELS

Prepared by:

A. H. Lange and L. P. Gieseler

ABSTRACT: Boundary-layer transition on a slender cone was observed at various Mach numbers between 1.9 and 4.2 in the NOL Supersonic Wind Tunnels No. 2 and 3. The Reynolds number of transition was found to be different in the two tunnels. A decrease of Reynolds number of transition with increasing Mach number was observed in the range of Mach numbers investigated. For a fixed Mach number, the transition Reynolds number could be lowered by introducing upstream disturbances in the wind-tunnel supply section. From the results of this investigation the conclusion is drawn that the slender cone is a suitably sensitive standard model to indicate differences in the free stream disturbance level of supersonic wind-tunnel flows. The tests also show that flow disturbances in the subsonic part of a tunnel are propagated through the Laval nozzle in a way to affect the transition in the boundary layer of a model placed in the supersonic stream.

U. S. NAVAL ORDNANCE LABORATORY
WHITE OAK, MARYLAND

i
UNCLASSIFIED

UNCLASSIFIED
NAVORD Report 2752

NAVORD Report 2752

19 February 1953

Data on the boundary-layer transition on a standard model are presented and conclusions are drawn regarding the relative disturbance level in two NOL supersonic tunnels. The investigation is exploratory in character, but is of practical importance for the correlation of wind-tunnel data taken in different facilities, and for the correlation between wind tunnel and flight.

The work was initiated in November, 1951 by the authors and Mr. J. L. Potter who was at that time with NOL. Negotiations concerning the use of the model at other wind-tunnel facilities in the country are planned. The authors wish to thank Mr. R. K. Squires who participated in the tests, and Mr. R. T. Schroth who designed the model.

EDWARD L. WOODYARD
Captain, USN
Commander

H. H. KURZWEG, Chief
Aeroballistic Research Department
By direction

UNCLASSIFIED
NAVORD Report 2752

CONTENTS

	Page
I. Introduction	1
II. Equipment	2
III. Test Procedure and Evaluation	4
IV. Results	6
V. Conclusions	9
VI. Notation	10
VII. References	11

ILLUSTRATIONS

Figure 1. Cone Model.
Figure 2. Profile of First Version of Cone.
Figure 3. Mean Free Path versus Mach number in Wind Tunnels with Atmospheric Supply.
Figure 4. Intake Section of Tunnels 2 and 3.
Figure 5. Regions of Laminar and Turbulent Boundary-Layer Flow on Standard Cone Model, Luminescent Lacquer Technique.
Figure 6. Typical Schlieren Picture of Transition in the Boundary Layer of the Standard Cone Model.
Figure 7. Comparison of Transition Reynolds Number in Tunnels No. 2 and 3.
Figure 8. Transition Reynolds Number in Tunnel No. 2 at Various Mach Numbers.
Figure 9. Variation of Reynolds Number of Transition with Mach Number for Bodies of Revolution.
Figure 10. Effect of Screens Located in Subsonic Part of Tunnel No. 3 on Reynolds Number of Transition, $M = 3.25$.

MEASUREMENT OF BOUNDARY-LAYER TRANSITION ON A
STANDARD MODEL TO DETERMINE THE RELATIVE DISTURBANCE
LEVEL IN TWO SUPERSONIC WIND TUNNELS

I. INTRODUCTION

1. It is well known that the turbulence level of the airflow in a wind tunnel affects boundary-layer transition (reference 1). It is important, therefore, to know the free stream turbulence level of a wind tunnel in order to make correct interpretation of wind-tunnel data.
2. While the technique of directly measuring free stream turbulence in subsonic flows is well mastered, it is in its first stages in supersonic flows and direct measurements are very difficult (reference 2). A standard model technique, comparable in scope to the standard sphere technique which had been common in subsonic wind tunnels before the development of hot wire anemometry (references 1 and 3), was therefore used to deduce information on the free stream disturbance level of the airflow in two of the NOL supersonic tunnels.
3. A 5° total apex angle cone, about 50 cm long and 4.5 cm in diameter at the base, served as the standard model. Transition in the boundary layer of the cone was determined by two methods, the luminescent lacquer technique and spark-schlieren photography, the latter method being used in the majority of the tests. Details of the model and of the two methods will be given in sections II and III.
4. The cone was chosen as a standard model for the following reasons:
 - (a) The head shock wave can be made weak by choosing small cone angles. Its influence on the boundary-layer transition is thereby minimized.
 - (b) The pressure is constant along the cone surface in supersonic flow. The influence of a pressure gradient on the boundary-layer transition is therefore eliminated.
 - (c) The boundary-layer transition can be determined optically; the hazards of probe interference are thereby eliminated. On a two-dimensional model this would not be feasible because of transverse contamination.

UNCLASSIFIED
NAVORD Report 2752

(d) The laminar boundary layer in supersonic conical flow has been treated theoretically, and experimental transition data are of interest in the analysis.

5. The tests supplied information on:

(a) The transition Reynolds numbers in the Aeroballistics Tunnels No. 2 and the Aerophysics Tunnel No. 3 under approximately equal tunnel supply conditions at Mach numbers 3.25 and 4.25,

(b) The Reynolds numbers of transition as a function of Mach number in Tunnel No. 2. The data were taken at Mach numbers 1.87, 2.15, 2.87, 3.25, and 4.25,

(c) The effect of disturbances introduced by screens in the subsonic portion of the wind tunnel on the transition Reynolds numbers in Tunnel No. 3 at Mach numbers 3.25 and 4.25.

6. Incidental information was obtained on:

(d) The effect of the two methods used for detecting transition,

(e) The effect of model imperfection, and

(f) The effect of a boundary-layer trip on transition.

II. TEST EQUIPMENT

(a) Wind Tunnels

7. The NOL Aeroballistics Wind Tunnel No. 2 has a 40 x 40 cm open test section. The supply air is taken from the atmosphere through a drier and straightener. The operation is intermittent and blows up to 1 minute duration can be made.

8. The NOL Aerophysics Wind Tunnel No. 3 has a 18 x 18 cm closed test section. The supply air is also taken from the atmosphere through a drier but no straightener is in the supply duct. The operation of the tunnel is continuous.

9. Both tunnels are described in more detail in reference 4.

(b) Model

10. Details of the model are shown in Figure 1. The first tests were made with a chromium plated brass cone which we will call "first version". Its surface had been ground before plating in a number of lengthwise sections while the model

UNCLASSIFIED
NAFORD Report 2752

was supported near the tip of the cone. The blending of these sectional grinds was not smooth. Figure 2 shows the deviations of the surface of this model from an ideal cone surface.

11. When the "second version" was manufactured the model was held at the cylindrical part only and the entire conical surface was machined in one continuous travel of the grinding wheel. This produced a true conical surface with a .03 mm radius point. The second version was also made of brass and no plating was applied.

12. The surface roughness of the second version was recorded with a Brush Surface Analyzer, Type PA 2. The record showed an average roughness of 0.25 microns, with occasional roughness elements as high as 1.0 microns. (One micron = 39.4 microinches). This value is given here that the roughness may be compared with that of models measured with the same type of instrument at other laboratories. It is felt that the quantitative indication of the instrument is a relative measure of the roughness only, because the radius of the tip of the stylus that feels along the surface is considerably larger than the indicated roughness.

13. The authors estimate that the roughness may actually be larger than indicated. However, even then the surface roughness may not be affecting transition at Mach numbers above the order of 2.5 as can be seen from the following considerations. Figure 3 is a plot of the mean free path of the molecules in the air stream vs. Mach number for a tunnel with atmospheric supply. Two curves are shown. One curve gives the mean free path near the surface of the model, assuming a temperature recovery factor $r = 0.9$. The other curve gives the mean free path in the free stream. The curves were determined from the equations

$$L = 9.29 \cdot 10^{-6} \left(1 + \frac{8-1}{2} M^2\right)^{\frac{1}{8-1}} [cm] \text{ (free stream)},$$

and

$$L_w = L \left(1 + r \cdot \frac{8-1}{2} M^2\right) [cm] \text{ (wall)}.$$

UNCLASSIFIED
NAVORD Report 2752

which were derived from elementary kinetic theory (reference 5) on the assumption of a supply pressure of 760 mm Hg and a supply temperature of 293°K. The measured peak surface roughness of 1 micron is shown to scale as a horizontal line in Figure 3. It is evident that a roughness which is even two to three times larger, is of the order of the mean free path for a Mach number of 2.5 and considerably smaller than the mean free path for all higher Mach numbers.

(c) Screens

14. The screens used in some tests in Tunnel No. 3 were placed in the 18 cm x 23.5 cm cross-section of the supply duct about 5 cm upstream from the nozzle blocks, that is, close to the beginning of the two-dimensional contraction leading to the nozzle throat (see Figure 4). The screens were made from commercial square wire mesh. The "coarse screen" had wires 0.097 cm in diameter, spaced 0.2 cm between centerlines, and the "fine screen" had wires 0.028 cm in diameter, spaced 0.16 cm between centerlines.

(d) Straightener in Tunnel No. 2.

15. The straightener in Tunnel No. 2 was located 200 cm upstream from the beginning of the supersonic nozzle in a 120 cm x 130 cm cross-section of the supply duct. It consisted of 0.05 cm thick sheet metal forming square tubes 4.6 cm on a side and 35 cm long (see Figure 4).

III. TEST PROCEDURE AND EVALUATION

16. Luminescent lacquer technique: This technique is described in reference 6*. In our case the model was spun rapidly around its axis of symmetry in a jig while it was sprayed with the lacquer in order to secure

* A lacquer which is a mixture of a carrier, a solvent, and luminescent particles is used. A coat of this lacquer viewed in ultra violet light looks light when dry and dark when wet. The higher rate of evaporation in the turbulent boundary layer of a model coated with the lacquer causes the lacquer to dry where the boundary layer of the model is turbulent long before it dries where the boundary layer is laminar, and those regimes are therefore clearly visible as light (turbulent) and dark (laminar) areas on the model.

UNCLASSIFIED
NAVORD Report 2752

uniform application. The model was then put into the tunnel and subjected to supersonic flow for a length of time just sufficient to dry the lacquer in contact with the turbulent boundary layer. Thereafter the model was taken from the tunnel and photographed from four sides in ultra violet light. Figure 5 shows some typical photographs. The method was abandoned later during the tests because of the unknown effect of the coating on the transition itself and the hazard that coatings of different thickness might influence the results by giving different Reynolds numbers of transition for equal ambient conditions.

17. Spark-schlieren photographs: Schlieren photographs of about 1 microsecond exposure time were taken of the model in the tunnel. The location of boundary-layer transition was then determined on the photographs as the point where the smooth outline of the laminar boundary layer breaks up into a turbulent structure. This point was considered as corresponding to the beginning of transition.

18. A typical test with the latter technique proceeded as follows: Using the continuous light source of the schlieren apparatus, the knife edge was put in a position nearly parallel to the model contour and adjusted while the wind tunnel was blowing until maximum contrast appeared at the boundary layer. Another blow was then made during which six flash photographs were taken in succession at about 3 second intervals. This procedure was then repeated after the knife edge had been rotated 180°. Since the boundary layer was visible on the upper and on the lower side of the model contour, the above procedure yielded in two blows 12 pictures with 24 values of the location of transition. A typical schlieren photograph is reproduced in Figure 6. Pictures taken with vertical knife edge adjustment and with the shadowgraph method were inferior.

19. The distance of the transition point from the tip of the cone, l , is used to compute the Reynolds number of transition,

$$Re = \frac{u \cdot l}{\nu}$$

where, u , is the velocity and, ν , is the kinematic viscosity of the undisturbed flow determined from nozzle calibrations.

UNCLASSIFIED
NAWORD Report 2752

20. Whenever a large number of test points was obtained for the same test condition, the results were treated in the following manner: The arithmetic mean, the largest value, and the smallest value were reported. In addition, the spread, s , of one half of the observations about a mean value was determined. This spread was determined from the equation

$$s = 0.8453 \frac{\sum i v_i}{\sqrt{n(n-1)}}$$

given, for instance, in reference 7. The equation is an approximate formula for the probable error of a single observation. The interval determined in this way is in our case not a measure of error but rather a measure of the amount that the Reynolds number of transition fluctuates with time. It is indicated as a thick vertical bar in the graphs, Figures 7, 8 and 10.

IV. RESULTS

21. Figure 7 shows a comparison of the Reynolds number of transition observed in tunnels No. 2 and 3. The ordinate is the Reynolds number of transition. The mean value, the total spread, and the spread of one-half of the values are shown for both tunnels. The number of values from which each plot was reduced is noted. The figure shows that the Reynolds number of transition is consistently about one million higher in tunnel No. 3 than in tunnel No. 2. The imperfect first version of the model gives the same qualitative behavior in both tunnels as the improved second version. However, the level of transition Reynolds numbers is reduced by approximately 1/2 million. The results at Mach number 4.25 are less conclusive than those at Mach number 3.25 because an important part of the model was invisible due to the presence of a steel rib in the tunnel sidewall. The value of the transition Reynolds number could only be bracketed between 1.6 and 2.0×10^6 for the boundary layer on the lower side of the cone. The upper side appeared laminar throughout.

22. It may be concluded from the higher Reynolds number of transition in Tunnel No. 3 that the disturbance level is lower there than in Tunnel No. 2 at Mach numbers 3.25 and 4.25. The lower turbulence level in Tunnel No. 3 may be caused by the absence of a straightener and the higher contraction ratio of this tunnel and the subsequent lower turbulence level in the intake.

UNCLASSIFIED
NAVORD Report 2752

23. The variation of Reynolds number of transition with Mach number in Tunnel No. 2 is shown in Figure 8. A decrease of Reynolds number of transition with increasing Mach number was observed.

24. In Figure 9 the results are compared with transition data obtained on other bodies of revolution. The curves of references 8 and 9 represent transition Reynolds numbers observed in the same tunnel. In reference 8 boundary-layer transition was observed in the same fashion as in the present report on a "Hollow Cylinder"; i.e., a tube with a sharp leading edge. Supersonic flow enters the tube and a weak shock is formed at the leading edge. The curve of reference 9 represents the Reynolds number at which the skin-friction drag of a cone-cylinder body of variable length increases suddenly. The curve denoted by "ogives NACA", reference 10, was obtained in a continuous wind tunnel on a slender ogive body with an extremely smooth surface. This curve too represents Reynolds numbers at which the sudden increase in skin-friction drag occurs (minimum of boundary-layer displacement thickness). Some single experimental points, found in the literature, references 11, 12, are also shown. The points denoted by triangles are the only non-wind-tunnel data of this graph. They were obtained from shadowgraphs of cone-cylinder bodies that were fired in the range of the Ballistics Research Laboratory, Aberdeen. Transition occurred in the conical forepart of the missiles. The data were taken from reference 13.

25. The NOL wind-tunnel data are in good agreement with each other. All show decreasing Reynolds numbers of transition with increasing Mach numbers. The same trend is exhibited by the NACA data at the lower Mach numbers. Decrease of the Reynolds numbers of transition with increase in Mach number is to be expected from boundary-layer stability theory, reference 14, in the wind tunnel where the ratio of wall temperature to equilibrium temperature is unity or, in an intermittent tunnel, slightly above unity ($T_w/T_e > 1$). To illustrate this the theoretical curves of minimum Reynolds number at which transition could occur, i.e., the Reynolds numbers of neutral stability of two-dimensional disturbances in the laminar boundary layer, are also shown for $T_w/T_e = 1$ and $T_w/T_e = 2$ in Figure 9. It is seen that the experimentally determined trend does not deviate decidedly from

UNCLASSIFIED
NAVORD Report 2752

the theoretical prediction. The large deviation in absolute value of 3 to 4 orders of magnitude must await further clarification. Although some deviation is to be expected, the combined effects of free stream turbulence and noise, surface roughness of the body, heat-transfer conditions in the boundary layer, and pressure gradient introduced by the model or inherent in the flow, can hardly explain the magnitude of the observed deviation.

26. An opposite trend, increasing Reynolds numbers of transition in the wind tunnel with increasing Mach numbers, is stated in reference 13. In the light of the evidence presented here and in the reference, such a trend appears doubtful. It is seen that even the range data, which should show this opposite trend due to the different heat-transfer situation, do not point it out clearly. However, the relative roughness of the constant absolute-roughness missiles increases with Mach number, which may account for this behavior.

27. Figure 10 shows the effect of screens placed in the subsonic supply duct of Tunnel No. 3 at $M = 3.25$. The coarse and the fine screen reduced the Reynolds number of transition by 1.2 and 1.1 million with respect to the case of no screen.

28. A comparison of the two methods used to determine transition showed that the methods agreed fairly well. The lacquer technique gave lower Reynolds numbers of transition than the spark-schlieren photographs but the averages never differed by more than 0.2 million. (All results shown in the graphs of this report are derived from spark-schlieren photographs).

29. The effect of model imperfections can be seen in the left half of Figure 7 where results obtained at $M = 3.25$ with the first and second versions of the model are shown. With the second version Reynolds numbers about 0.5 million larger are observed in both tunnels.

30. A small rubber O-ring put on the cone as a boundary-layer trip appeared to be ineffective at $M = 1.86$ and at $M = 4.25$ but lowered the Reynolds number of transition in the middle of the Mach number range $M = 2.83$ and 3.25 . However, the schlieren pictures were difficult to read and interpret, and results are therefore not presented in detail.

31. The surface temperature of the cone was not measured during the tests. It is slightly above recovery temperature in the intermittent Tunnel No. 2 and it is equal to recovery

UNCLASSIFIED
NAVORD Report 2752

temperature in the continuously operating Tunnel No. 3. In order to minimize the effect of a model temperature higher than equilibrium temperature, repeated blows were made in Tunnel No. 2 before the transition was determined. From earlier tests during which temperatures were measured on a cone-cylinder, it can be concluded that the transition Reynolds number is altered due to the remaining temperature deviation by less than 0.2 million.

V. CONCLUSIONS

32. The location of the boundary-layer transition on a slender cone has been shown to be influenced by:

- (a) The flow conditions of a particular tunnel.
- (b) The free stream Mach number.
- (c) Turbulent disturbances produced by screens in the subsonic portion of the tunnel.

33. As a result of the investigation, it can be concluded that the location of the transition is a measure of the disturbance level in the wind tunnel, and that the slender cone is a suitable model to indicate differences in disturbance level. Although we cannot completely rule out the influence of model temperature, it appears that Tunnel No. 2 has a higher disturbance level than Tunnel No. 3 at the same Mach number. Disturbances introduced in the subsonic portion of the tunnel appear in measurable magnitude in the supersonic flow. A decreasing Reynolds number of transition with increasing Mach number was observed. This, however, may be a specific feature of the type of wind tunnel in which a large change of free stream conditions accompanies a change in Mach number.

UNCLASSIFIED
NAVORD Report 2752

VI. NOTATION

- l - Distance from tip of cone to transition region.
- u - Free stream velocity.
- ν - Free stream kinematic viscosity.
- Re - Reynolds number of transition based on free stream properties.
- M - Free stream Mach number.
- T_0 - Supply temperature.
- T - Free stream temperature.
- T_w - Temperature on surface of model.
- T_E - $= r T_0 - (r-1)T$, Equilibrium temperature, temperature associated with zero heat transfer.
- r - $= (T_E - T)/(T_0 - T)$, temperature recovery factor.
- L - Mean free path of air molecules in the free stream.
- L_w - Mean free path of air molecules near the wall.
- n - Number of observations.
- s - Probable error of a single observation.
- v - Deviation of a measurement from the mean.
- γ - Specific heat ratio.

UNCLASSIFIED
NAVORD Report 2752

VII. REFERENCES

1. Prandtl, L., *Der Luftwiderstand von Kugeln*, Nachr. d.k. Gesellsch. f. Wiss., Goettingen, Math. Phys. Klasse (1914), p. 177.
2. Kovasznay, L. S. G., *Turbulence in Supersonic Flow*, Institute of the Aeronautical Sciences, 21st Annual Meeting, New York, 27 January 1953.
3. Dryden, H. L. and Kuethe, A. M., *Effect of Turbulence in Wind-tunnel Measurements*, NACA TR 342, 1929.
4. Lightfoot, J. R., *The Naval Ordnance Laboratory Aeroballistic Facility*, Naval Ordnance Laboratory Report 1079, 15 August 1950.
5. Kennard, E. H., *Kinetic Theory of Gases*, First Edition, McGraw-Hill, New York, (1938) pp. 97-115.
6. Stalder, J. R. and Slack, E. G., *The Use of a Luminescent Lacquer for the Visual Indication of Boundary-Layer Transition*, NACA TN 2263, January, 1951.
7. Mellor, J. W., *Higher Mathematics for Students of Chemistry and Physics*, Dover, New York, (1946), p. 524.
8. Lee, R. E., *Measurements of Pressure Distribution and Boundary-Layer Transition on a Hollow Cylinder Model*, NAVORD Report 2823, Naval Ordnance Laboratory, White Oak, Maryland, March 1953.
9. Potter, J. L., *New Experimental Investigations of Friction-Drag and Boundary-Layer Transition on Bodies of Revolution at Supersonic Speeds*, NAVORD Report 2371, Naval Ordnance Laboratory, White Oak, Maryland, April 1952.
10. Love, E. S., Coletti, D. E., and Bromm, A. F., National Advisory Committee for Aeronautics, Unpublished data, 9 x 9 inch Tunnel.
11. National Advisory Committee for Aeronautics, Unpublished data, 9 x 9 inch Tunnel.
12. Chapman, D. R., *An Analysis of Base Pressure at Supersonic Velocities and Comparison with Experiment*, NACA Report 1051, Washington, D. C., 1951.

UNCLASSIFIED
NAVORD Report 2752

- 13 Gazley, C Jr , Boundary-Layer Stability and Transition in Subsonic and Supersonic Flow, Journal of the Aeronautical Sciences, 20, 1, 19 January 1953.
- 14 Van Driest, E. R., Calculation of the Stability of the Laminar Boundary Layer in a Compressible Fluid on a Flat Plate with Heat Transfer. Journal of the Aeronautical Sciences, 19, 12, 801, December 1952.

NAVORD REPORT 2752

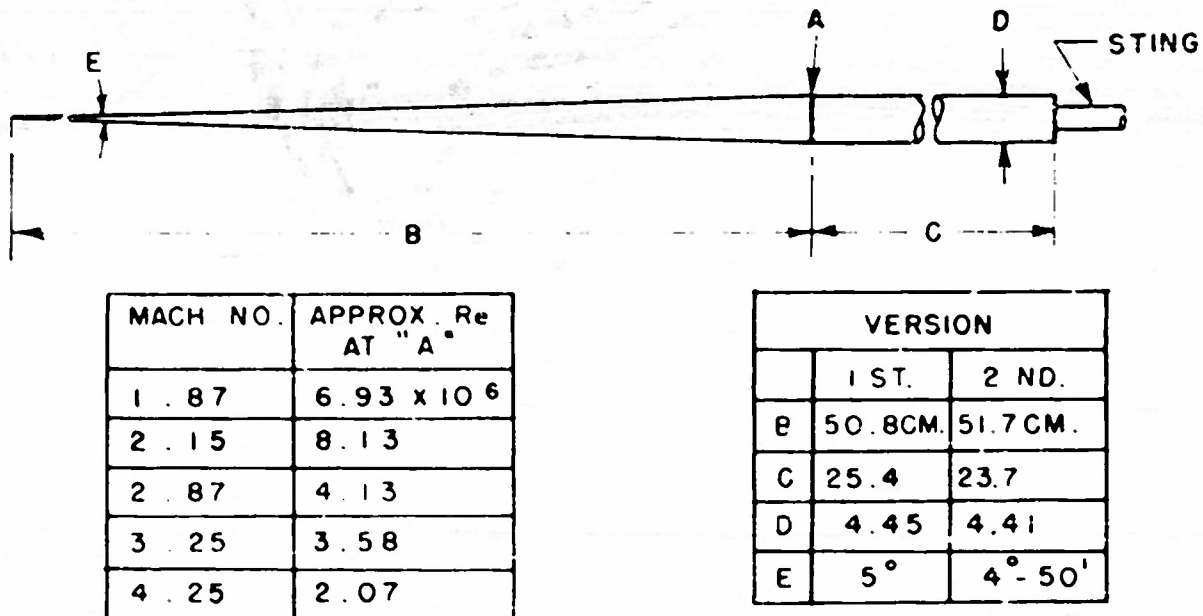


FIG. 1 CONE MODEL

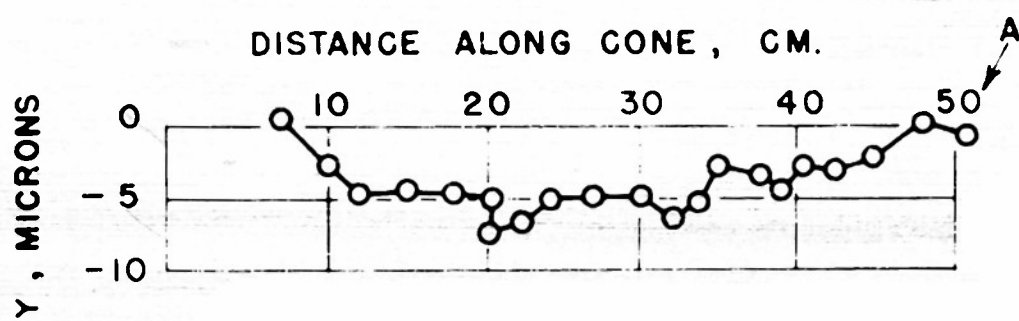


FIG. 2 PROFILE OF FIRST VERSION OF CONE

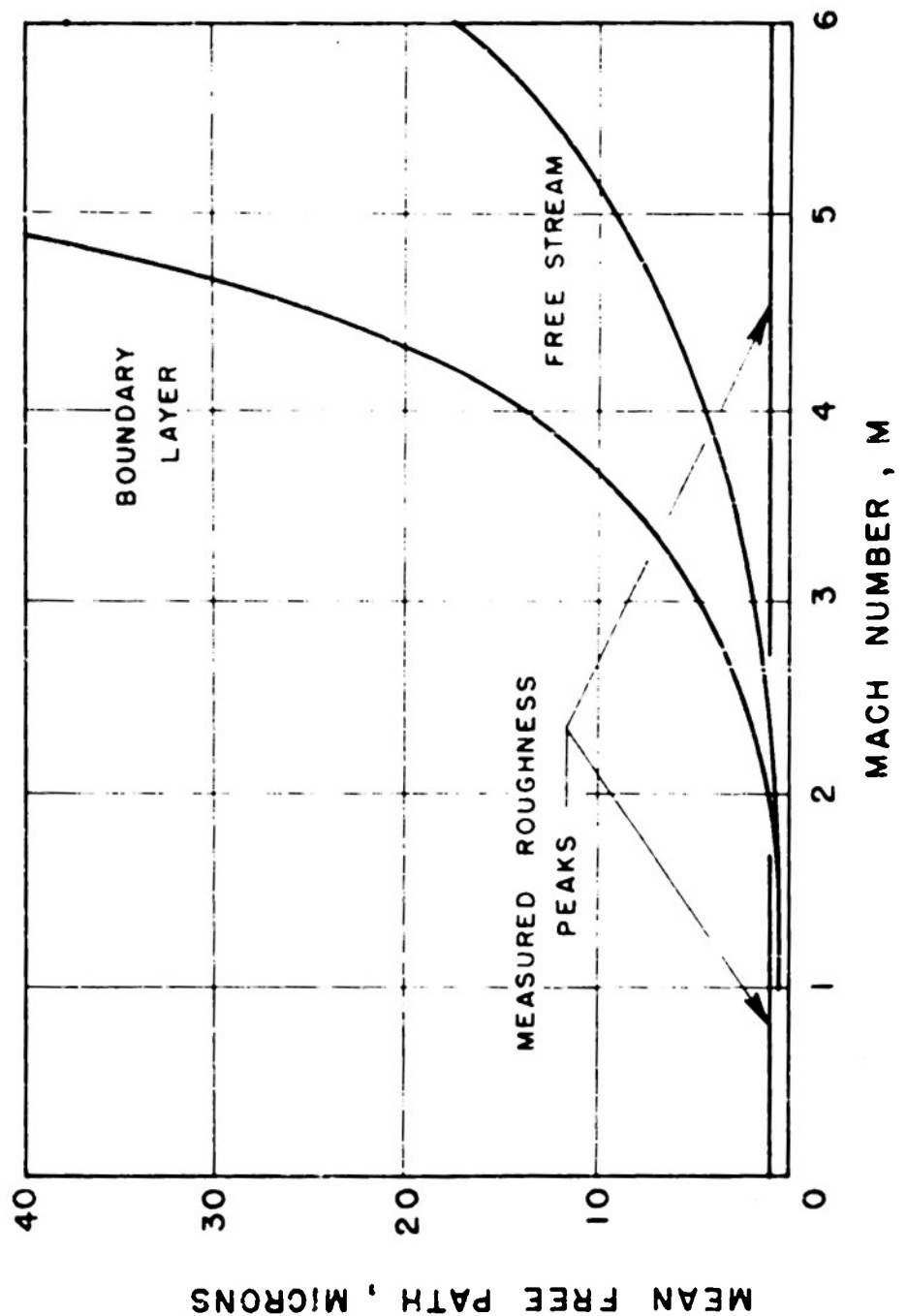


FIG. 3 MEAN FREE PATH VS. MACH NUMBER IN WIND
TUNNEL WITH ATMOSPHERIC SUPPLY

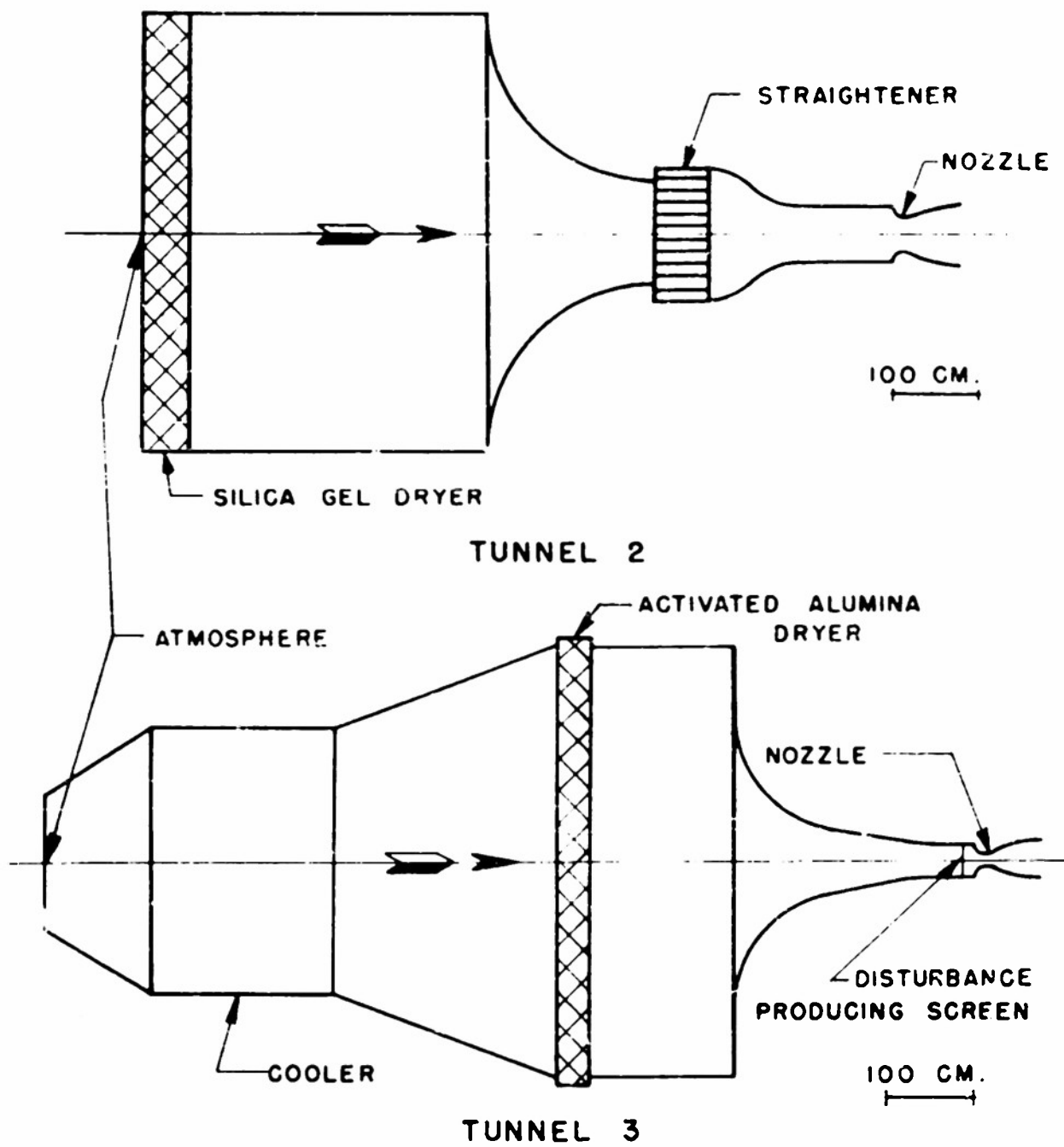
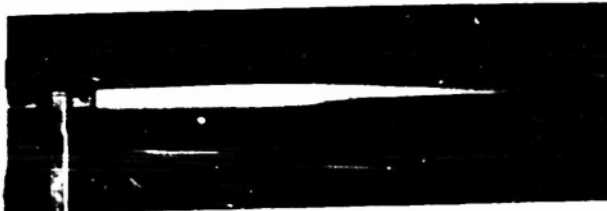
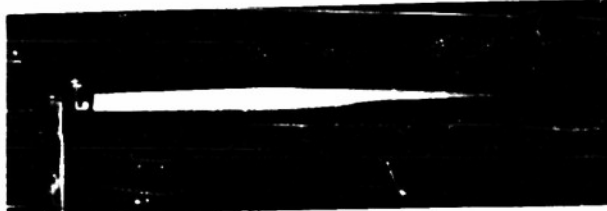
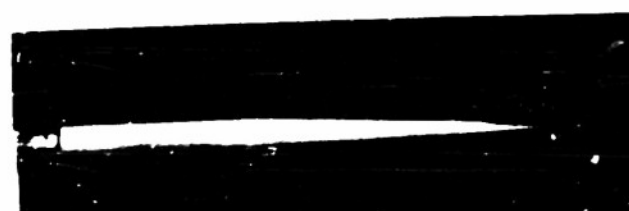
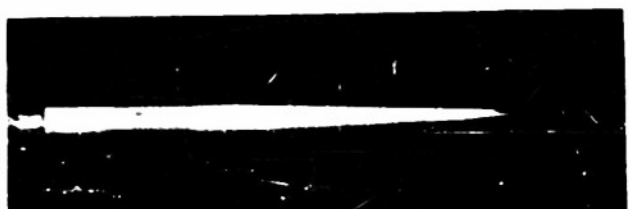


FIG. 4 INTAKE SECTION OF TUNNEL 2 AND 3

NAVORD REPORT 2752

MACH 3.25



→ MODEL IS SPINNING

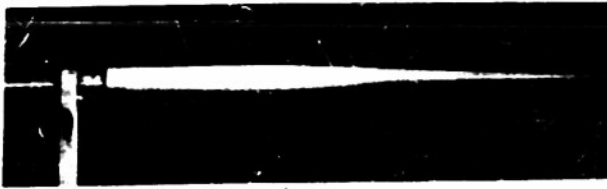
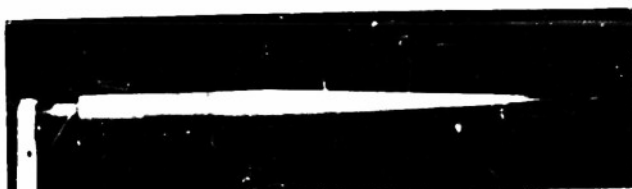
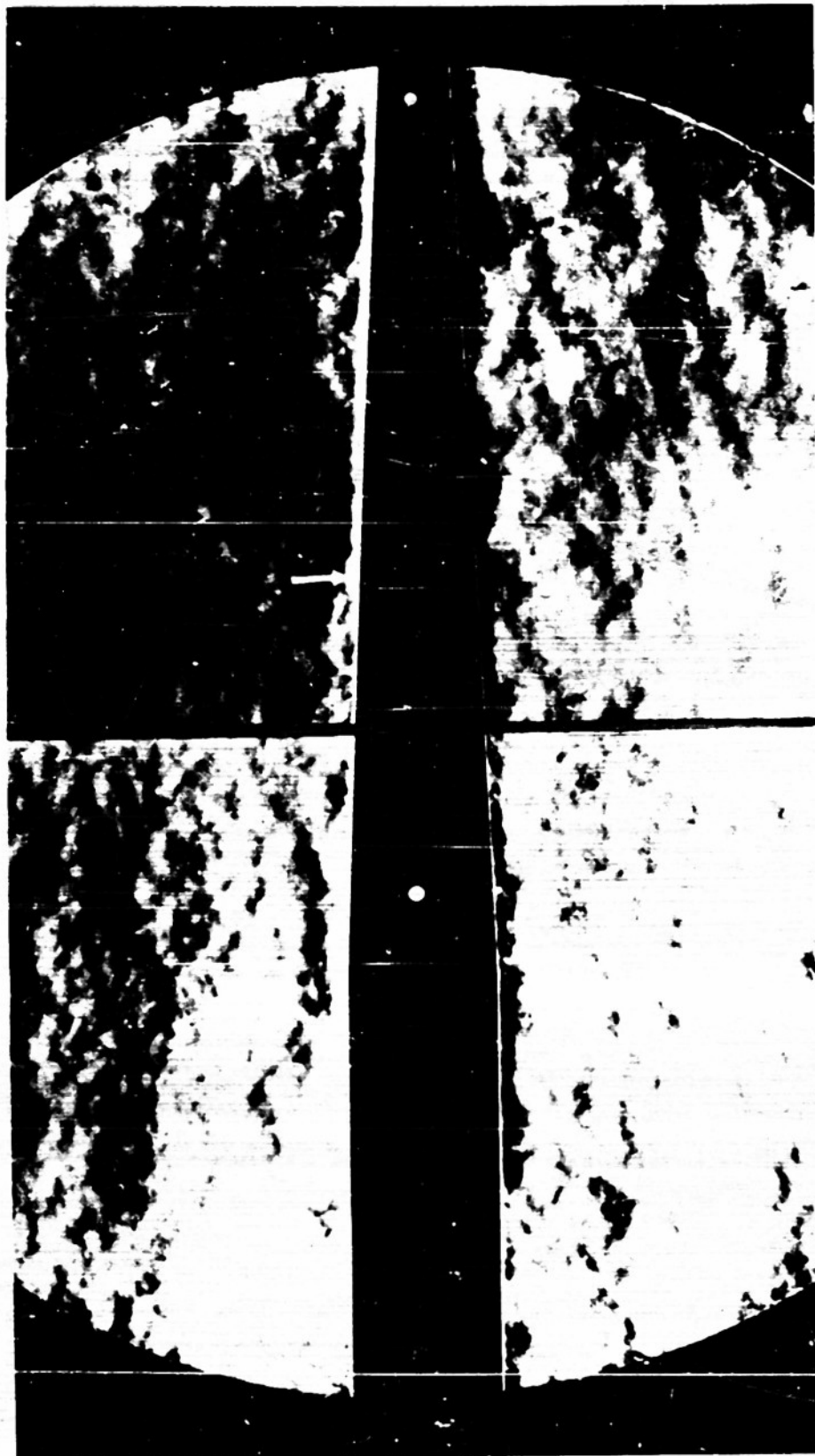


FIG. 5 REGIONS OF LAMINAR (DARK) AND TURBULENT (LIGHT) BOUNDARY LAYER FLOW ON STANDARD CONE MODEL, LUMINESCENT LAQUER TECHNIQUE.

NAVORD REPORT 2752



MACH 4.25, TUNNEL 2, $Re \sim 1.6 \times 10^6$, \downarrow INDICATES TRANSITION POINT
FIG. 6 TYPICAL SCHLIEREN PICTURE OF TRANSITION IN THE BOUNDARY LAYER
OF THE STANDARD CONE MODEL

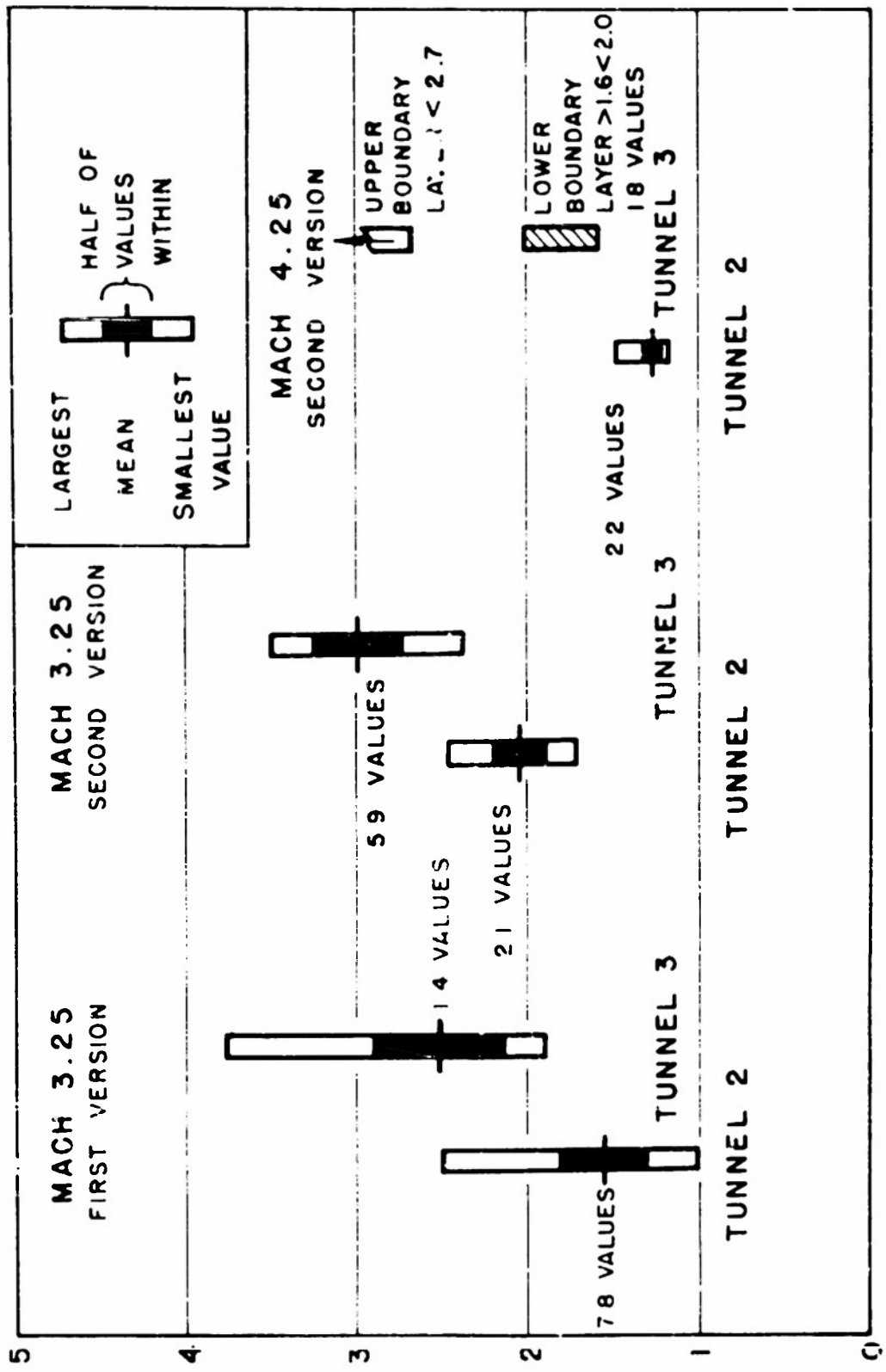


FIG. 7 COMPARISON OF TRANSITION REYNOLDS NUMBER IN
TUNNEL 2 AND 3

NAVORD REPORT 2752

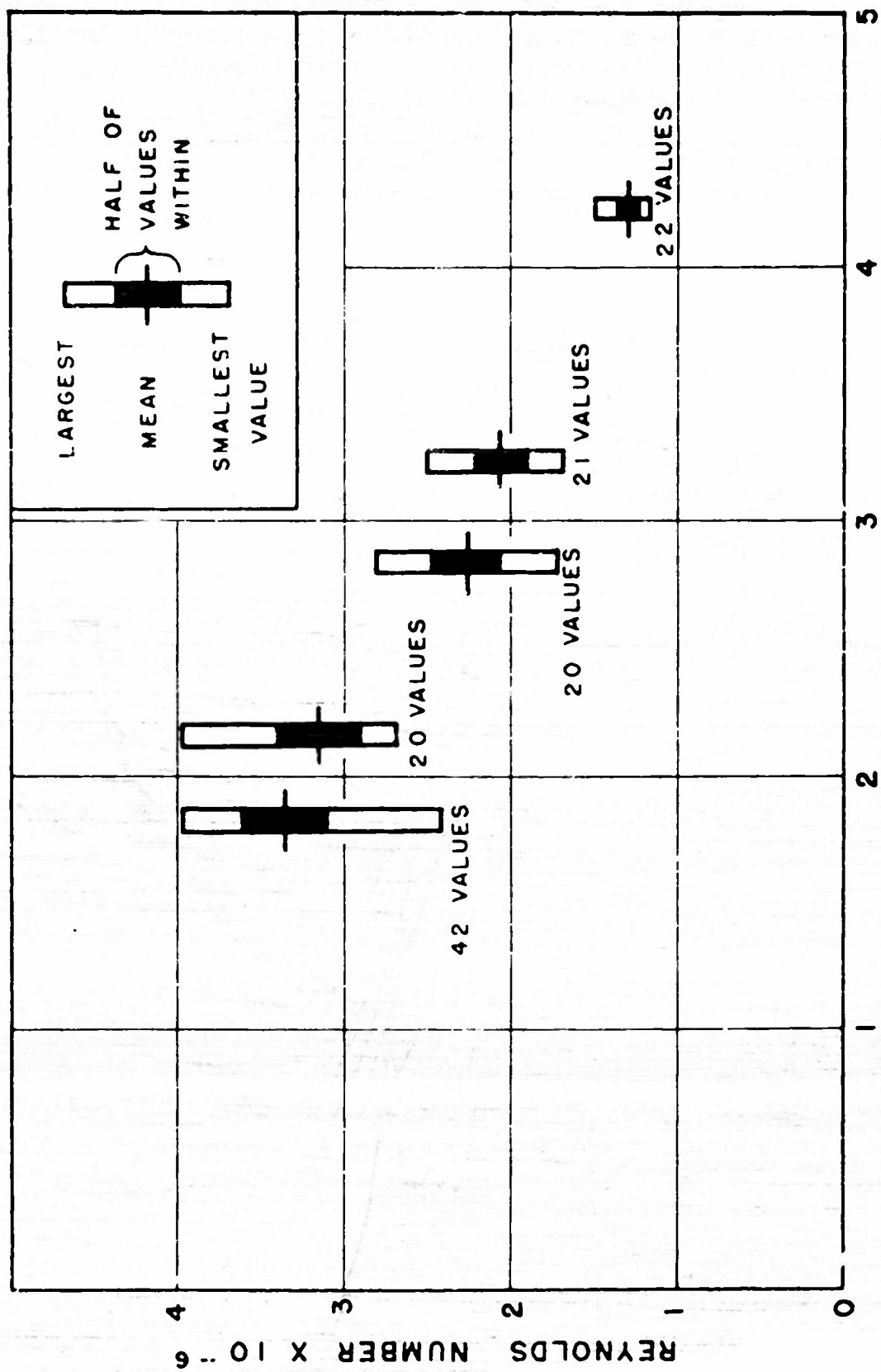


FIG. 8 TRANSITION REYNOLDS NUMBER IN TUNNEL 2
AT VARIOUS MACH NUMBERS

NAWORD REPORT 2752

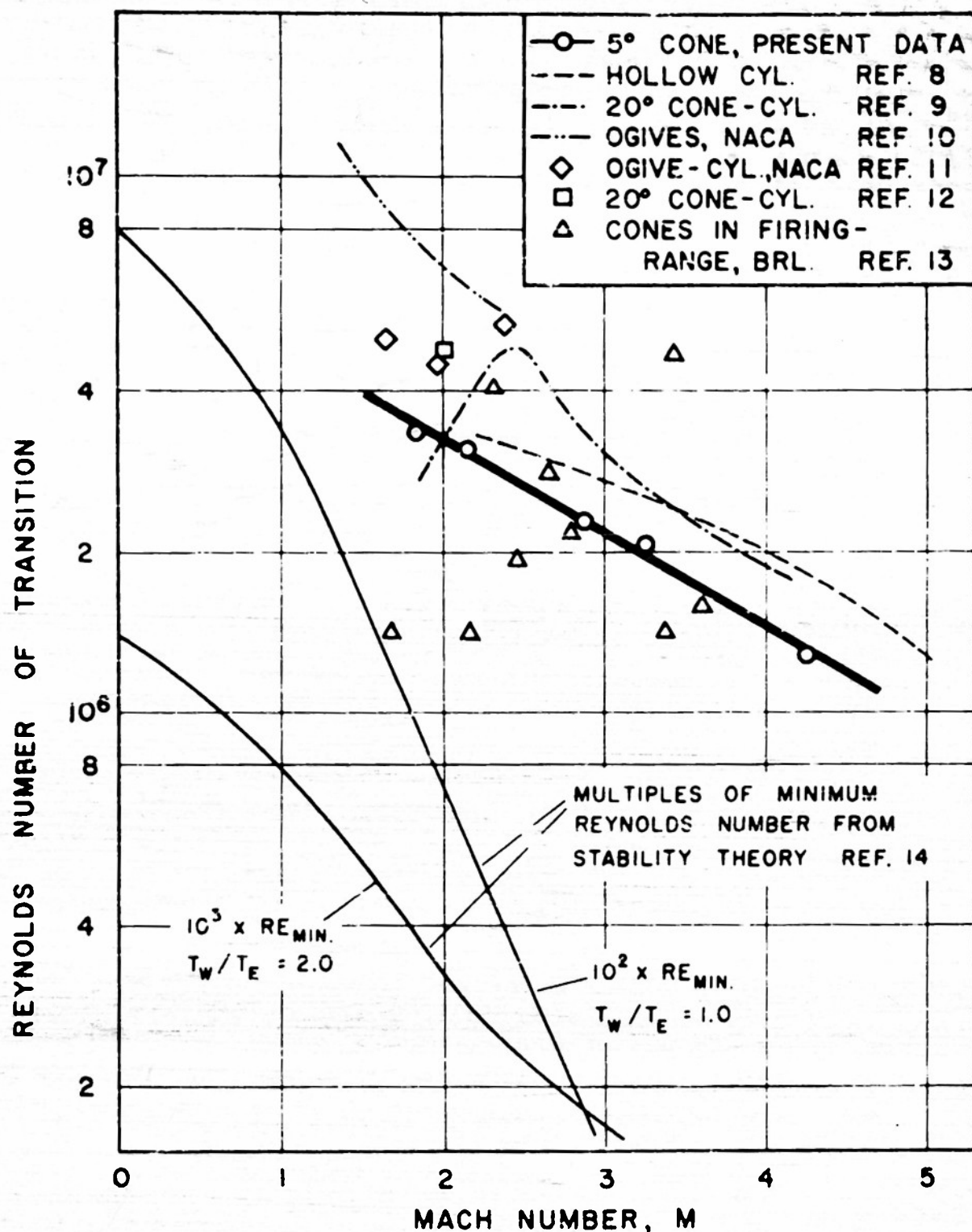


FIG. 9 VARIATION OF REYNOLDS NUMBER OF TRANSITION
WITH MACH NUMBER FOR BODIES OF REVOLUTION

NAVORD REPORT 2752

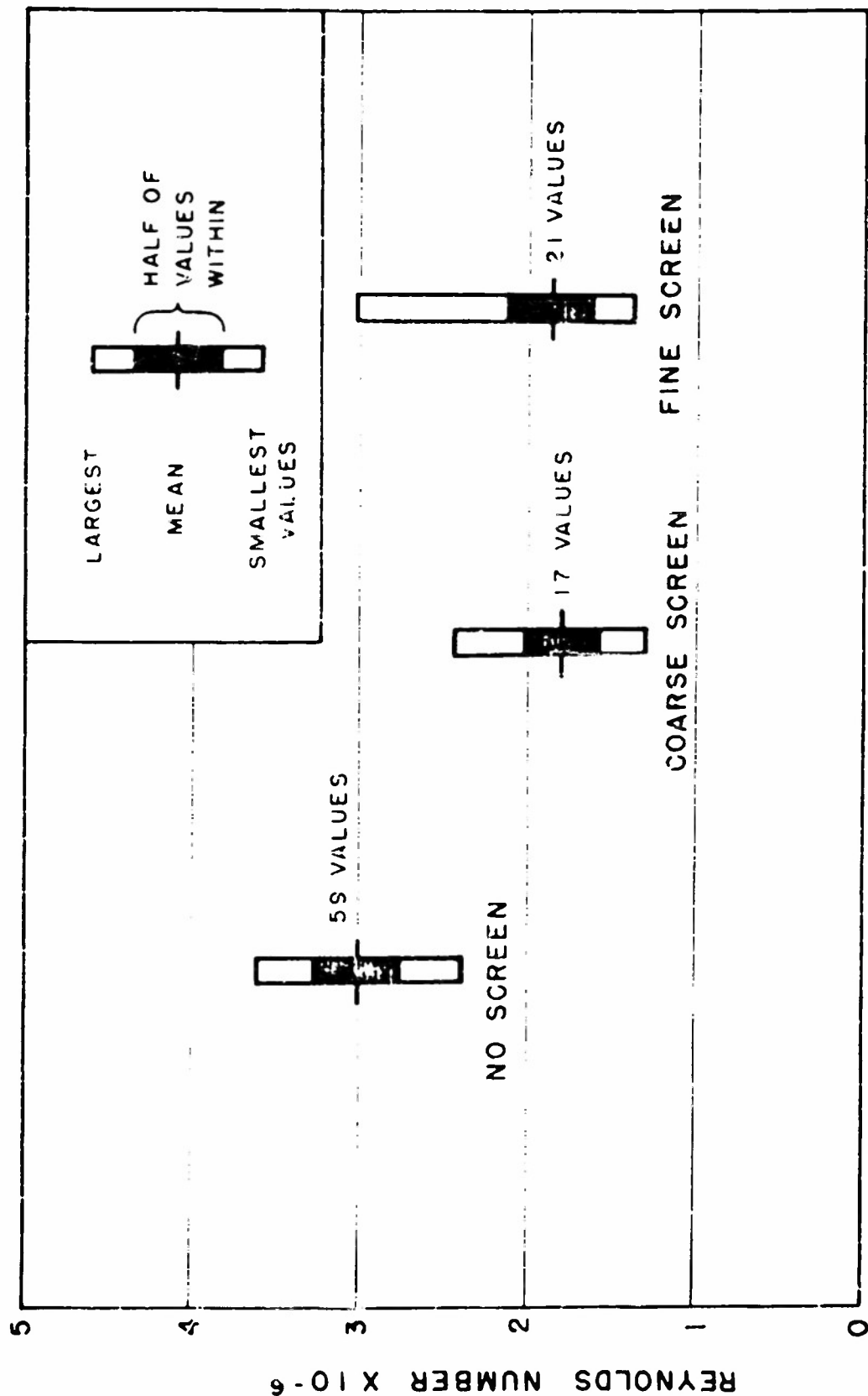


FIG. 10 EFFECT OF SCREENS LOCATED IN SUBSONIC PART OF TUNNEL 3 ON REYNOLDS NUMBER OF TRANSITION, $M = 3.25$

Aeroballistic Research Department
External Distribution List for Aeroballistics Research (Xla)

No of
Copies

6 Office of Naval Research
Branch Office
Navy 100
Fleet Post Office
New York, New York

1 Commanding General
Aberdeen Proving Ground
Aberdeen, Maryland
Attn: Dr. B. L. Hicks

1 National Bureau of Standards
Aerodynamics Section
Washington 25, D.C.
Attn: Dr. G. B. Schubauer, Chief

1 Ames Aeronautical Laboratory
Moffett Field, California
Attn: Walter G. Vincenti

1 University of California
Observatory 21
Berkeley 4, California
Attn: Leland E. Cunningham
VIA: InsMat

1 Massachusetts Inst. of Technology
Dept. of Mathematics, Room 2-270
77 Massachusetts Avenue
Cambridge, Massachusetts
Attn: Prof. Eric Reissner
VIA: InsMat

1 Graduate School Aeronautical Engr.
Cornell University
Ithaca, New York
Attn: W. R. Sears, Director
VIA: ONR

1 Applied Math and Statistics Lab
Stanford University
Stanford, California
Attn: R. J. Langle, Associate Dir.
VIA: Ass't InsMat

1 University of Minnesota
Dept. of Aeronautical Engr.
Minneapolis, Minnesota
Attn: Professor R. Hermann
VIA: Ass't InsMat

1 Case Institute of Technology
Dept. of Mechanical Engineering
Cleveland, Ohio
Attn: Professor G. Kuettner
VIA: ONR

1 Harvard University
109 Pierce Hall
Cambridge 38, Massachusetts
Attn: Professor R. von Mises

**Aeroballistic Research Department
External Distribution List for Development (X2)**

<u>No. of Copies</u>		<u>No. of Copies</u>	
	Chief, Bureau of Ordnance Department of the Navy Washington 25, D. C.		Research and Development Board Library Branch Pentagon 3D1041
1	Attn: Rea	2	Washington 25, D. C.
1	Attn: Rexe		
1	Attn: Re3d		
3	Attn: Re4a		
	Chief, Bureau of Aeronautics Department of the Navy Washington 25, D. C.		Chief, AFSWP P. O. Box 2610 Washington, D. C.
1	Attn: AER-TD-414	1	Attn: Technical Library
2	Attn: RS-7		
	Commander U.S. Naval Ordnance Test Station Inyokern P.O. China Lake, California		Chief, Physical Vulnerability Branch Air Targets Division Directorate of Intelligence Headquarters, USAF
2	Attn: Technical Library	1	Washington 25, D. C.
	Commander U.S. Naval Air Missile Test Center Point Mugu, California		The Artillery School Antiaircraft and Guided Missiles Br
3	Attn: Technical Library	2	Fort Bliss, Texas Attn: Research and Analysis Sec.
	Superintendent U.S. Naval Postgraduate School Monterey, California		Commanding General Wright Air Development Center Wright-Patterson Air Force Base
1	Attn: Librarian	8	Dayton, Ohio Attn: WCAPD
	Commanding Officer and Director David Taylor Model Basin Washington 7, D. C.	2	Attn: WCRR
1	Attn: Hydrodynamics Laboratory	1	Attn: WCSD
	Chief, Naval Research Navy Research Section Library of Congress Washington 25, D. C.	5	Attn: WCSO
2			
	Chief, Naval Operations Department of the Navy Washington 25, D. C.		Director Air University Library Maxwell Air Force Base, Alabama
1	Attn: Op-51		
	Office of Naval Research Department of the Navy Washington 25, D. C.		Commanding General Aberdeen Proving Ground Aberdeen, Maryland Attn: C. L. Poor
2	Attn: Code 463		
	Director Naval Research Laboratory Washington 25, D. C.		National Bureau of Standards Washington 25, D. C.
1	Attn: Code 2021 Code 3800	1	Attn: Librarian (Ord. Dev. Div.)
		1	Attn: W. Ramberg
	Officer-in-Charge Naval Aircraft Torpedo Unit U.S. Naval Air Station Quonset Point, Rhode Island		National Bureau of Standards Corona Laboratories (Ord Dev. Div.) Corona, California Attn: Dr. H. Thomas
1			
	Office, Chief of Ordnance Washington 25, D. C.		National Bureau of Standards Building 3U, U.C.L.A. Campus 405 Hilgard Avenue Los Angeles 24, California Attn: Librarian
1	Attn: ORDTU		
			University of California Berkeley 4, California Attn: Mr. G. J. Maslach
		1	Attn: Dr. S. A. Schaaf
			California Inst. of Technology Pasadena 4, California Attn: Librarian (Guggenheim Aero. Lab.) VIA: BuAero

<u>No. of Copies</u>	<u>No. of Copies</u>
1	University of Michigan Willow Run Research Center Ypsilanti, Michigan Attn: L.R. Bassell VIA: InsMat
1	University of Minnesota Rosemount, Minnesota Attn: J. Leonard Frame VIA: Ass't InsMat
1	The Ohio State University Columbus, Ohio Attn: G.L. VonEschen VIA: Ass't InsMat
1	Polytechnic Institute of Brooklyn 99 Livingston Street Brooklyn 2, New York Attn: Dr. Antonio Ferri VIA: ONR Branch Office
1	Princeton University Forrestal Research Center Library Project Squid Princeton, New Jersey
2	Massachusetts Inst. of Technology Project Meteor Cambridge 39, Massachusetts Attn: Guided Missiles Library
1	Applied Physics Laboratory The Johns Hopkins University 8621 Georgia Avenue Silver Spring, Maryland Attn: Arthur G. Norris Technical Reports Office VIA: NIO
1	Armour Research Foundation 35 West 33rd Street Chicago 16, Illinois Attn: Engr. Mechanics Division VIA: ONR Branch Office
1	Defense Research Laboratory University of Texas Box 1, University Station Austin, Texas VIA: InsMat
2	Eastman Kodak Company Navy Ordnance Division 50 West Main Street Rochester 4, New York Attn: Dr. Herbert Trotter, Jr. VIA: NIO
	General Electric Company Building #1, Campbell Avenue Plant Schenectady, New York Attn: J.C. Hoffman VIA: InsMachinery
	The Rand Corporation 1500 Fourth Street Santa Monica, California Attn: The Librarian VIA: InsMat
	Consolidated Vultee Corporation Dangerfield, Texas Attn: J.E. Arnold, Manager VIA: Dev. Contract Office
	Douglas Aircraft Company, Inc. 3000 Ocean Park Boulevard Santa Monica, California Attn: Mr. E.F. Burton VIA: BuAero Resident Rep.
	North American Aviation, Inc. 12214 Lakewood Boulevard Downey, California Attn: Aerophysics Laboratory VIA: BuAero Rep.
5	National Advisory Committee for Aero. 1724 F Street Northwest Washington 25, D. C. Attn: Mr. E. B. Jackson
1	Ames Aeronautical Laboratory Moffett Field, California Attn: H. Julian Allen
2	Attn: A.C. Charters
1	Theoretical Aerodynamics Division Langley Aeronautical Laboratory Langley Field, Virginia Attn: Theoretical Aerodynamics Div
1	Attn: Dr. A. Busemann
2	Attn: J. Steele
1	NACA Lewis Flight Propulsion Lab. Cleveland Hopkins Airport Cleveland, Ohio Attn: Dr. John C. Evvard
1	Hughes Aircraft Company Culver City, California Attn: Dr. Allen E. Puckett
1	Institute of Aerophysics University of Toronto Toronto 5, Ontario Attn: Dr. Gordon N. Patterson, Dir. VIA: BuOrd (Ad8)